A SECOND-ORDER JAHN–TELLER DISTORTION IN THE SOLID: THE PHASE TRANSITION IN VS$_x$*

JÉRÔME SILVESTRE, WOLFGANG TREMEL and ROALD HOFFMANN

Department of Chemistry and Materials Science Center, Cornell University, Ithaca, NY 14853 (U.S.A.)

Summary

Tight-binding band structure calculations have been performed on both the NiAs (hexagonal) and MnP (orthorhombic) structures of vanadium sulfide VS. A band folding procedure is used to generate the electronic structure of the hexagonal phase in orthorhombic symmetry and allows one to understand the reasons for the NiAs to MnP structural distortion as vanadium vacancies in VS are filled. When a critical electron filling of the metal d bands is reached, a second-order Jahn–Teller mixing operates to stabilize the MnP structure and induces the concomitant formation of metal–metal zig zag chains. The resulting "dip" in the density of states at the Fermi level is analyzed in conjunction with the experimentally observed changes in conductivity, and Knight shift measurements. Finally, the computed relative stability of the two structures for different metal monosulfides is shown to agree qualitatively with the experimental data available.

1. Introduction

Establishing logical ties between the structural chemistry and the physical properties of solid state materials is often a difficult but challenging task. Intimately related is the question of how electronic factors affect and even tune the structure of a compound in the solid state. As it turns out, a small change in temperature, pressure and/or chemical composition may alter drastically the properties, whether chemical or physical, of the material under consideration.

A nice illustration of this delicate balance is provided by vanadium monosulfide in the neighborhood of the 1-to-1 stoichiometry. More than 20 years have now elapsed since Franzen and Westman [1] first recognized that VS$_x$ (x close to 1) could crystallize in the orthorhombic MnP-type structure. At that time this result appeared to conflict with a previous [2] structural determination which had concluded that VS adopted the related but more symmetrical hexagonal NiAs structure. The reported [1] absence of a two-

---

*Dedicated, with admiration, to Professor J. D. Corbett on the occasion of his 60th birthday.

phase region and a more detailed study [3] of VS_x ($x \approx 1$) led to the remarkable conclusion that a subtle change in the stoichiometry actually triggers a second-order [4] phase transition between the NiAs and MnP forms of VS_x.

A schematic summary of the room-temperature results is presented in 1; when the ratio V:S reaches a critical value (0.94), the structure undergoes a continuous displacive distortion which converts the hexagonal structure to the orthorhombic one. As can be deduced from 1 the perfectly stoichiometric material (V:S = 1) is found to crystallize in the MnP structure. However, the material "switches" [5] to the NiAs form at about 550 °C.

NiAs | MnP — V/S
0.94
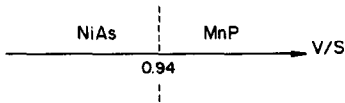
1

Numerous physical measurements were carried out on VS_x as a function of x and temperature so as to include the transition point: electrical conductivity and magnetic susceptibility [5], lattice constants [3, 5] and Knight shift [6] measurements. An increase of the density of state (DOS) at the Fermi level on going from the MnP to the NiAs structure was proposed to account for the observed changes [5]. Furthermore, the use of crystal data for different sulfur contents x allows one to plot the valence electron concentration (VEC) as a function of x; it was shown [3] that the NiAs-to-MnP transition occurs when the VEC reaches a critical value (0.3 electrons $Å^{-3}$), suggesting in turn that the morphological change is controlled in some way by the electron filling around the Fermi level ϵ_F. Within this context, it is important to realize that an increase in V:S means a decrease in the formal oxidation state of each vanadium, or equivalently a higher electron filling of the metal d bands. To put it in a different way, on reading 1 from left to right the number of d electrons on each vanadium atom increases.

Previous band calculations have been performed on the hexagonal phase of VS and nicely accounted for the electrical and mechanical properties of the solid [7, 8]. We should also point out here a discussion of the distortion in terms of a charge density wave instability, presented by Liu *et al.* [9].

In this work, we aim at an understanding of the actual electronic driving force for the phase transition. Our purpose is also to analyze the induced alterations in the electronic structure and tie them up with the formation of metal–metal zigzag chains (*vide infra*) and the observed changes in physical properties on transition.

Tight-binding band structure calculations within the extended Hückel framework were carried out for both the NiAs and MnP structures of VS. The computational and geometrical details are listed in Appendix A.

2. The topology of the NiAs → MnP distortion

The NiAs structure **2** consists of hexagonal close packed layers which alternate metal and non-metal atoms. (The space group is $P6_3/mmc$ [10], $a = 3.33$ Å; $c = 5.87$ Å.) An easy way to visualize the atomic arrangement of VS in this phase is to look down the c axis of the three-dimensional structure; the picture is that shown in **3a**. Starting with a hexagonal layer of vanadium atoms at $z = 0$, one finds at $z = \frac{1}{4}$ a layer of sulfur atoms, then a layer of vanadium at $z = \frac{1}{2}$ superimposable on that at $z = 0$ and finally a second layer of sulfur atoms at $z = \frac{3}{4}$. The pattern is repeated along the c

● Ni
○ As

2

$P6_3/mmc$

● V at z=0.0
○ V at z=0.5
○ S at z=0.25
⊛ S at z=0.75

3a

Pnma

3b
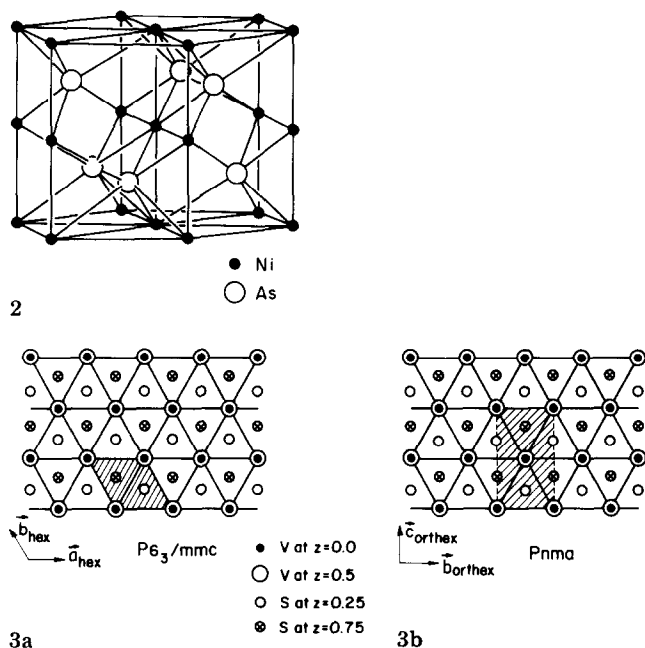
direction to generate a three-dimensional stacking of the type AbAcAbAc... Each sulfur sits at the center of a trigonal prism defined by the vanadium atoms which in turn are octahedrally coordinated to 6 sulfurs. The V–S distances in this structure are typical of coordination compounds. There is no S···S bonding, but the V···V contacts are reasonably short, indicating d band formation with substantial dispersion. The axial V···V separation, that along $\tilde{c}$, is shortest at 2.94 Å. The V···V contacts within the hexagonal net are longer, 3.33 Å.

The cross-hatched area of **3a** defines the projection of the three-dimensional unit cell on the plane perpendicular to c. Clearly the content of the primitive cell is twice the formula unit, i.e. two vanadium and two sulfur atoms. For reasons which will become apparent shortly, it is useful to view

the *same* structure from a different perspective and in particular to double the contents of the cell to emphasize the pseudo-orthorhombic symmetry of the structure. Taking the short axis as b (*Pnma* setting), **3b** defines the orthohexagonal unit cell. The relationship between the translation vectors of the two settings is: $a_{orthex} = -c_{hex}, b_{orthex} = a_{hex}, c_{orthex} = a_{hex} + 2b_{hex}$. In other words, the number of layers perpendicular to the plane of the paper does not change [3] and the doubling of the cell volume is brought about by the doubling of the area within that plane. The unit cell thereby defined contains four atoms of each kind.

The reason we double the unit cell is that it is then much easier to derive the MnP structure from the NiAs one. Let us start from the doubled cell defined in **3b** and redrawn in **4a**. The distortion from NiAs to MnP takes **4a** into **4b**, looking down the a axis. We emphasize here the motion (arrows

4a   4b
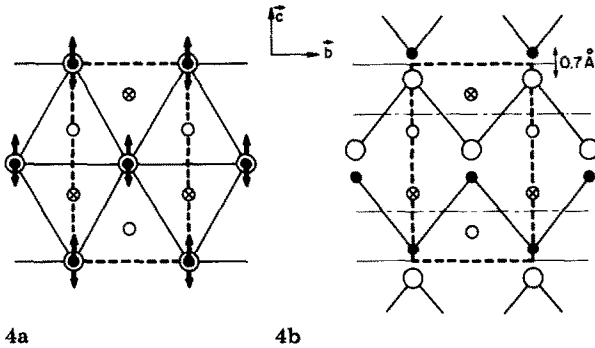
in 4a) within the (b, c) plane since it gives rise to the most drastic changes in the structure. However, one should also point out that a slight shift of the atoms occurs along the a direction as well; however, the magnitude of the a direction shift is only about 15% that of the shift within the (b, c) plane. In particular the picture **4b** is somewhat idealized since it suggests that a two-fold axis is present at $c = \frac{1}{2}$. In reality this axis is absent due to the above-mentioned displacements along the a axis. If one focuses on a pair of metal atoms initially in a kind of eclipsed configuration in **4a**, they are now separated along c_{ort} by about 0.7 Å, see **4b**. One of the remarkable features of the distortion is that the overall dimensions of the orthohexagonal cell are basically conserved after the transformation to the orthorhombic structure: $a_{orthex} = 5.87$ Å, $a_{ort} = 5.85$ Å; $b_{orthex} = 3.33$ Å, $b_{ort} = 3.31$ Å; $c_{orthex} = 5.77$ Å, $c_{ort} = 5.83$ Å. (The values for the orthohexagonal cell are derived from the values quoted above: $a = 3.33$ Å, $c = 5.87$ Å [10]. Those for the orthorhombic structure were extracted from ref. 11.)

Topologically, the primary effect in the NiAs → MnP transformation [12] may be seen as the rupture of every hexagonal net of metal atoms to form zigzag chains, as depicted in **5**. Before distortion, the metal–metal
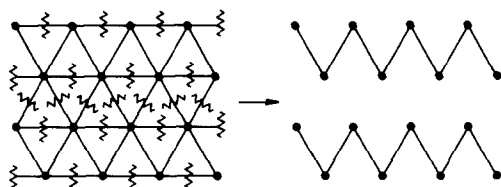
5

contacts are 3.33 Å within the net whereas the bond length of each V–V bond within the chains is about 2.76 Å. Interestingly enough the metal–metal distances in the perpendicular direction do not change much, 2.94 Å *versus* 3.00 Å.

3. The hexagonal phase

Figure 1 shows the calculated band structure for VS in the NiAs structure. The symmetry lines [13] are labelled according to the nomenclature of the insert in the upper right corner of the Fig. 1, which outlines the shape of the three-dimensional hexagonal Brillouin zone (BZ).

Recalling that the cell contains two vanadium and two sulfur atoms, one recognizes the six sulfur p bands between −16.1 and −11.0 eV, the s bands being buried below −18.0 eV. The 10 metal d bands spread over about 6 eV. The lowest ones remain relatively flat throughout the zone except along Γ–A, the direction of the short V–V contact. These bands are essentially V–S non-bonding. The upper bands show some dispersion, undoubtedly via V–S through-bond coupling. The same argument applies for some of the sulfur p centered bands. Overall the shape of the band structure compares rather favorably with that obtained [7] by Liu and coworkers using an *ab initio* technique. They do observe a little more mixing between sulfur and vanadium bands which will translate into a slight difference in the charge density distribution. Our calculations point to less covalent character in the V–S linkages.

The DOS curve is shown in Fig. 2 and was computed with the use of the special k-points technique. The Fermi level ϵ_F falls at −8.15 eV. Notice that the d states split roughly into two peaks with the Fermi level lying almost in between. All this agrees qualitatively with the photoelectron spectrum obtained by Franzen and Sawatzky [14] on $V_{0.92}S$ and gives us some confidence in the relevance of the computations. From Fig. 2 it is clear that VS should exhibit metallic conductivity and in fact it does. Returning to the band structure of Fig. 1, one can see that ϵ_F sits in the middle of relatively flat bands, conferring on VS its magnetic properties [5, 15].
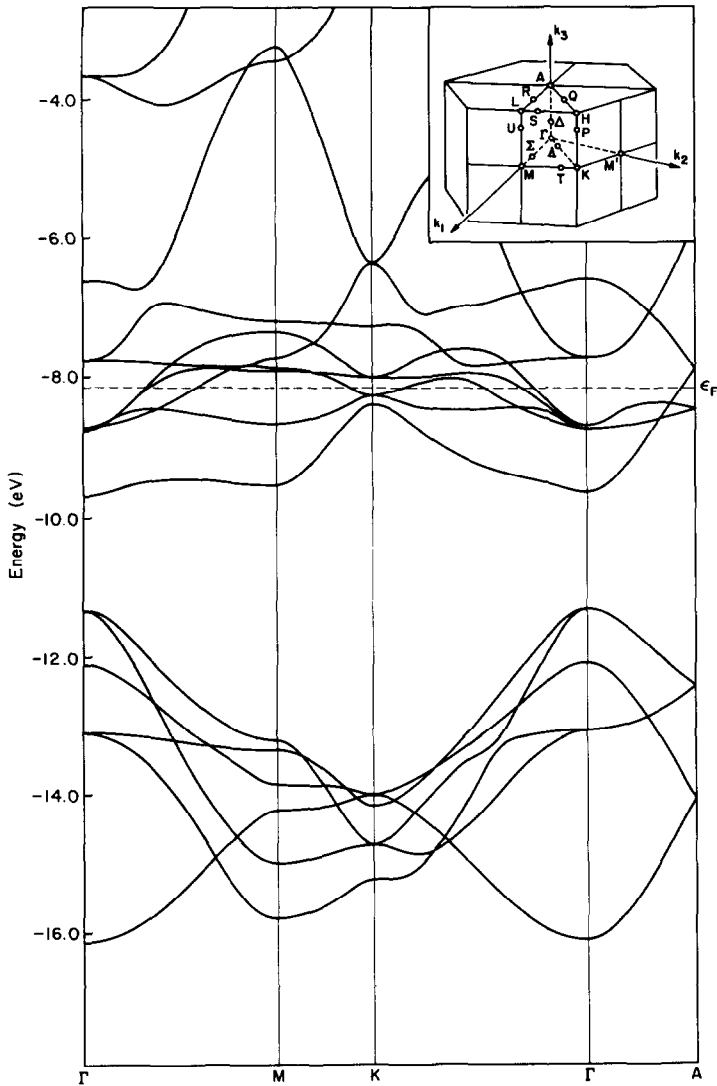
Fig. 1. The band structure of VS in the NiAs geometry.

4. The electronics of the distortion

In order to pin down the electronic driving force for the distortion, some "preparative" work is necessary. Specifically the idea is to construct the electronic structure of the hexagonal phase in the lower orthorhombic symmetry, *i.e.* prepared for the distortion.

The band structure of the undistorted phase in orthorhombic symmetry may be obtained using a band folding procedure [16] and the band structure generated in hexagonal symmetry, *i.e.* that shown in Fig. 1.
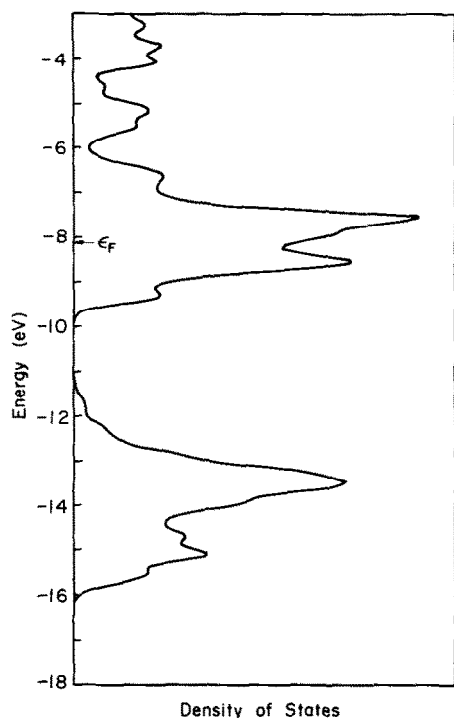
Fig. 2. Density of states of VS in the NiAs geometry.

As noted earlier the orthohexagonal cell has a volume twice that of the hexagonal cell. Also, it was mentioned that this doubling comes about in the plane perpendicular to the c axis of the hexagonal structure. Thus in the following we confine our attention to the two-dimensional problem of generating the band structure of a rectangular lattice from that of a hexagonal structure twice as small. Going into reciprocal space this size relationship is reversed [17, 18] and the BZ of the rectangular lattice is contained within that of the hexagonal one, and is twice as small. This is shown in 6 where the rectangular BZ is defined by the broken line. The area enclosed within the triangle ΓMK is the irreducible wedge of the

6
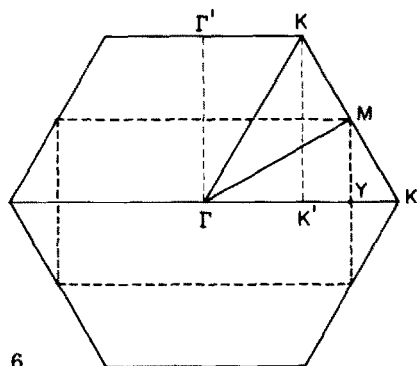
hexagonal BZ. The band structure along ΓM, MK and KΓ was indeed computed and presented in Fig. 1. The purpose is now to construct the bands along ΓY, Y being at the boundary of the rectangular BZ. The choice of this specific line is dictated by the fact that the forthcoming distortion occurs along this direction in direct space.

One can clearly use the bands along the ΓK line but not all the way; the section YK belongs to the next rectangular BZ and must be folded back to produce the YK' piece. We have used here both the time reversal symmetry and the translational property existing in reciprocal space. Another justification for this procedure is that the plane perpendicular to that of the paper and containing the MY line is a symmetry element in reciprocal space. Finally the MK line is equivalent to the Γ'K line (rotation by $\pi/3$) which in turn is translated back to ΓK' in the irreducible wedge of the rectangular lattice. In summary, the bands along ΓY are generated by folding the bands along Γ-K-M of Fig. 1, so that the points Γ and M overlap with each other. An obvious consequence of this construction is the number of bands along ΓY, twice the number of those present in Fig. 1. This is hardly surprising, since the orthohexagonal cell contains twice as many atoms as the hexagonal one.

Figure 3 shows the result of applying this procedure for the metal d bands in the −10 to −6 eV energy window. Perhaps we should discuss briefly here a technical point: on folding, point K emerges as point K', see 6. However, the former, as the end point of the line ΓK in hexagonal symmetry, requires a zero derivative for all the bands (see Fig. 1). Point K', however, is not a special point in the rectangular BZ, and the bands *do not* have a vanishing derivative at this point, which falls at two-thirds of the ΓY line away from Γ.

The band structure of Fig. 3 exhibits a multitude of level crossings. However, we can predict which will actually be removed (or transformed into avoided crossings) as the geometrical distortion to the MnP structure 5 is introduced. These "evanescent" crossings are circled in Fig. 3. They are easily identified when the bands are labelled according to their properties with respect to symmetry elements present in the *distorted* system, namely a 2_1 screw axis and a glide plane. The former propagates the zigzag chain whereas the latter takes one such chain into the next one along the orthorhombic a axis, see 4b. Upon distortion, one also anticipates the splitting of the degeneracies at Γ, since here the group of the wavevector k goes from D_{6h} to D_{2h} and the latter excludes irreducible representation of dimension greater than one. In contrast, the degeneracies at Y should remain due to the non-symmorphic nature of the group of k along this line.

The crucial features of the band structure shown in Fig. 3 are the crossings just below −8.0 eV, extremely close to our Fermi level for VS. The NiAs structure is actually observed for a stoichiometry such that ϵ_F probably lies slightly below these crossings. When vanadium vacancies are filled, and the number of d electrons thereby increased, then ϵ_F will go up and hit one of the two crossings. The structure distorts, the crossings become avoided and most of the *filled* levels are stabilized.
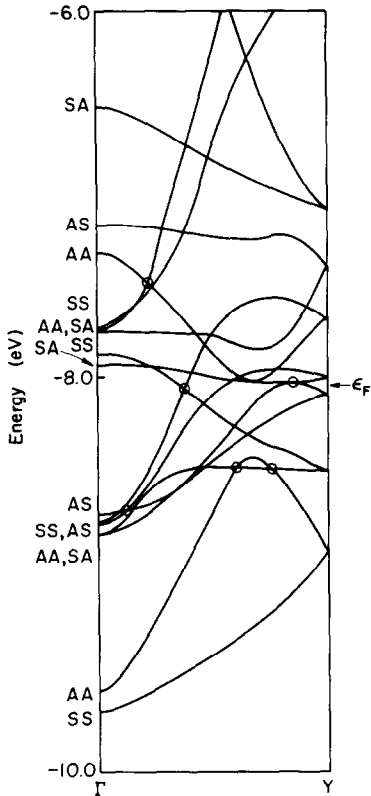
Fig. 3. Folded band structure from ΓMK (Fig. 1) to produce ΓY in the orthorhombic Brillouin zone.

Figure 4 shows both the band structure of the undistorted system (left) and that obtained from a calculation on the distorted one, the MnP phase. All the expected features are present: splitting of degeneracies at Γ and avoided crossings. We emphasize the SA–AS pairs (thick lines) because those are responsible for the stabilization and the nature of the distortion. It is rewarding to focus specifically on the zone edge, point Y. The initially tiny gap between the third and fourth degenerate pairs ③ and ④ is increased enormously on distortion. These bands become ②' and ③' respectively. The lowest band, ③ → ②', is much stabilized and is filled. The top band (④ → ③') remains basically at the same energy; this is due to the fact that the overall mixing involves all the four pairs of symmetry type SA–AS. One may visualize this process best by plotting a Walsh diagram along the distortion at Y. This is done in Fig. 5. The solid lines correspond to the SA–AS pairs, whereas the dashed ones refer to SS–AA pairs. The Fermi level for stoichiometric VS falls somewhere just below −8.0 eV; its exact position depends strongly on the accuracy of the calculations and on the particular stoichiometry under consideration.
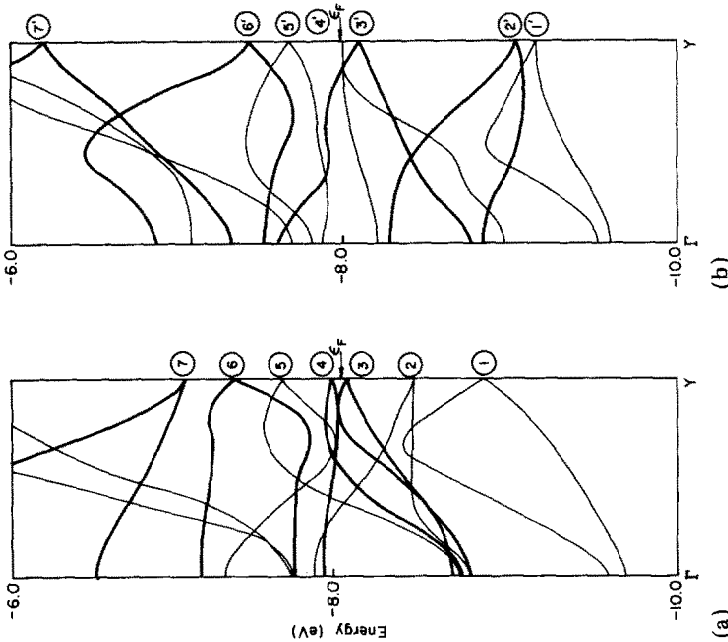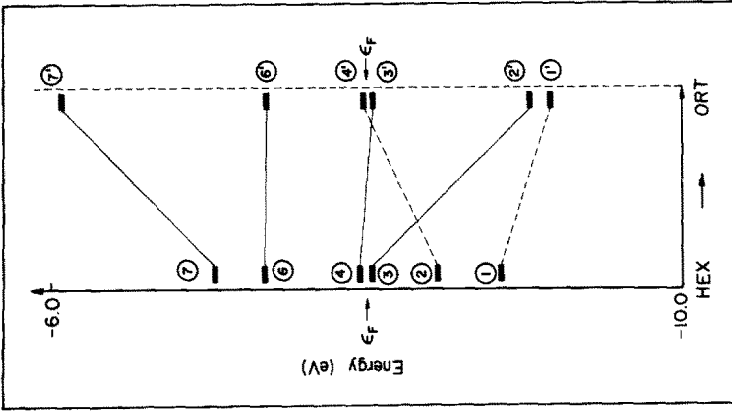
Fig. 4. Band structure along ΓY for the orthohexagonal cell of the NiAs structure (left) and the orthorhombic cell of the MnP structure (right). Heavy lines are SA/AS pairs.

Fig. 5. A Walsh diagram at Y for the four SA–AS pairs of bands (solid lines) and the lowest two SS–AA pairs of bands (broken lines). Each level is doubly degenerate.

The SA/AS pairs undergo a typical multi-orbital type interaction with the lowest band stabilized, the next two remaining basically unaltered, while the top band carries most of the destabilization. Notice also that the two SS/AA pairs are also somewhat split in the process, ①and ② emerging as ①' and ④'.

The energetic driving force for the distortion is a mixing of empty bands into filled bands, made allowed by a lowering in symmetry. This is reminiscent of a second-order Jahn–Teller effect [19], except that in the solid the mixing takes place along *a full line* in reciprocal space, as witnessed by the plots of Fig. 4.

What about the actual geometry of the distortion? To tackle this question one has to take a rather close look at the exact composition of the crystal orbitals involved. This is conveniently done at Y, the wavefunction there being real. We can furthermore concentrate on orbitals centered on pairs of atoms within one hexagonal layer since the second pair of metal atoms in the next layer is related to the original pair by the glide plane.

In 7b are drawn the SA and AS crystal orbitals at Y, corresponding to point ④ in Fig. 4a. These are mainly d_{yz} in character and degenerate. One is bonding within the unit cell (broken lines) whereas strong antibonding exists between different unit cells, since we are at the zone edge here. The other combination, conversely, is antibonding within the cell but bonding between adjacent cells. Orbitals are sketched only on a one-dimensional subset of atoms of the hexagonal lattice specified in 7a. Clearly, these bands are

7
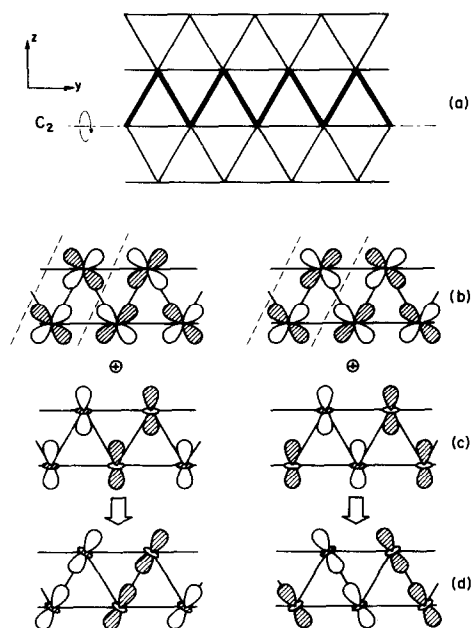
antisymmetric with respect to the 2-fold axis shown in **7a**, present in the hexagonal structure.

The orbitals at point ③ of Fig. 4(a) are shown in **7c**. We have extracted the d_{z^2} components out of the total wavefunctions. Now the bands are *symmetric* with respect to the C_2 axis. On distortion of the hexagonal structure to the orthorhombic symmetry, the C_2 axis is lost. These two sets of bands are thus allowed to mix, since each set consists of an SA and an AS band, the symmetry labels referring to the 2_1 screw and the glide plane. Following the usual rules of perturbation theory the upper set (**7b**) mixes in a bonding way into the lower one (**7c**), to generate two bands with the topology outlined in **7d**. A net decrease in antibonding and increase in bonding ensue and drive the formation of the zigzag chain. The two orbitals shown in **7d** are obviously degenerate and correspond to those of point ②′ in Fig. 4(b). Notice that a half filling of bands **7d** should produce a pairing and disrupt the zigzag chain. A related phenomenon occurs in metal mono-phosphide structural chemistry [20].

Interestingly enough the break-up of the hexagonal net of vanadium atoms displays features similar to cases where a true Peierls distortion takes place; in the present situation, one can view the pairing as one taking a two-dimensional framework into subsets of one-dimensional lattices. A rigorous Peierls distortion occurs at one point of the BZ (the edge) and splits one band into two subbands [21]. In contrast, the phase transition in VS_x is driven by mixing between different bands.

Returning to Fig. 4, it is apparent that the density of levels around and below the -8.0 eV mark changes upon distortion. We confirmed that point by a plot of the DOS for both the NiAs and the MnP structures of VS.

Figure 6 shows the result in the -10 to -6 eV energy range. The mixings discussed previously create a "dip" in the DOS curve of the MnP
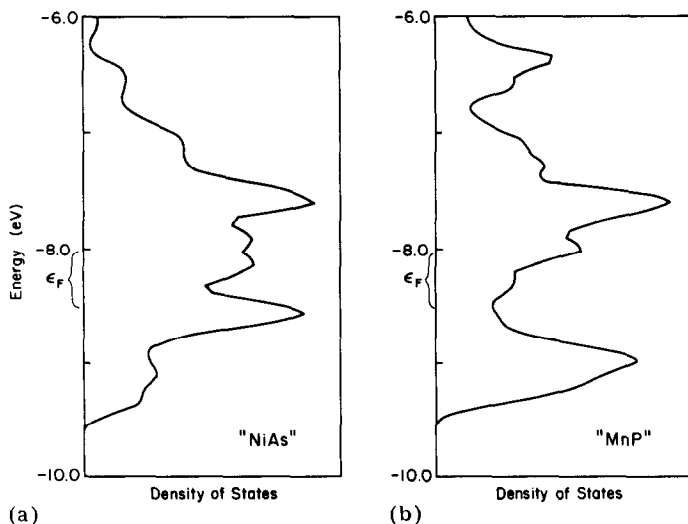
Fig. 6. Density of states for the NiAs (left) and MnP (right) structure of VS. The braces locate the range of ϵ_F in the neighborhood of the 1-to-1 stoichiometry.

geometry just below —8.0 eV. The DOS at the Fermi level is decreased on going from the NiAs to the MnP phase of VS_x. This conclusion agrees with that anticipated by Franzen and Wiegers [5] on the basis of conductivity measurements. Similarly a decrease of $N(\epsilon_F)$ on going from the hexagonal to the orthorhombic structure could explain the observed [6] decrease in Knight shift when the system undergoes the phase transition.

In this closing section we would like to "feed" more electrons into the system and compare the stability of the NiAs and MnP phases as a function of the electron count. Within this rigid band model approximation the relative stability of the two structures is shown in 8. The horizontal axis counts
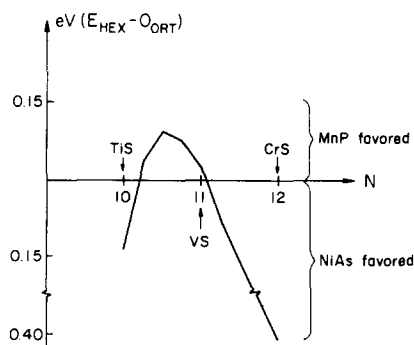
8

the number of valence electrons per formula unit. Thus $N = 10$ corresponds to TiS, $N = 11$ to VS, $N = 12$ to CrS. The vertical axis measures the difference in energy per cell between the hexagonal and orthorhombic structures. The curve indicates that somewhere in between titanium and vanadium the MnP structure should become more stable. Furthermore, moving to the right from vanadium the NiAs phase should become more stable again. With the formalism of counting each sulfur as S^{2-}, every point on the horizontal axis corresponds to a d electron count on the metal. For example a d^2 system (TiS) is predicted to be in the hexagonal structure whereas the d^3 compound ($VS_{1.00}$) is more stable in the MnP geometry. Reaching a d^4 metal atom pushes the NiAs structure back to lower energy relative to its MnP counterpart. These results agree well with the experimental information available, since TiS and CrS crystallize [22, 23] in the NiAs structure whereas $VS_{1.00}$ adopts the MnP geometry. One can take a further step and compute from 8 the critical d electron count which converts the two structures: we find $d^{2.25}$. Experimentally the phase transition was initially shown to occur for $VS_{1.06}$ which translates into a $d^{2.88}$ electron configuration for the vanadium atom. A more accurate titration study on $Ti_xV_{1-x}S$ demonstrated later that $d^{2.34}$ was closer to reality [24]. We believe that the agreement with our value is good enough, given the approximate nature of the computations.

5. Conclusions

In this contribution we have proposed an electronic reason for the phase transition occurring in vanadium monosulfide. The creation of sulfur vacancies makes the Fermi level rise up to a critical value where empty and filled bands are particularly prone to mix so as to stabilize the structure and generate metal–metal zigzag chains. The modification of the density of states which ensues can account qualitatively for the observed changes in physical properties. The type of distortion at work in VS_x turns out to govern the structural differences in metal monophosphides as well [20]. In these systems, however, increasing the number of d electrons gives rise to a Peierls distortion which eventually breaks the metal–metal chains. A detailed report on that topic is in preparation [25].

Acknowledgments

References

1 H. F. Franzen and S. Westman, *Acta Chem. Scand.*, *17* (1963) 2353.
2 W. Biltz and A. Köcher, *Z. Anorg. Allg. Chem.*, *241* (1939) 324; E. Hoschek and W. Klemm, *Z. Anorg. Allg. Chem.*, *242* (1939) 49.
3 H. F. Franzen and T. J. Burger, *J. Chem. Phys.*, *49* (1968) 2268.
4 L. D. Landau and E. M. Lifshitz, *Statistical Physics*, Pergamon Press, London, 1959, Chap. 4. See also, H. F. Franzen, Second order phase transitions and the irreducible representation of space groups, *Lect. Notes Chem.*, Vol. 32, Springer-Verlag, Berlin, 1982; H. F. Franzen, C. Haas and F. Jellinek, *Phys. Rev. B*, *10* (1974) 1248.
5 H. F. Franzen and G. A. Wiegers, *J. Solid State Chem.*, *13* (1975) 114.
6 H. F. Franzen, D. M. Strachan and R. G. Barnes, *J. Solid State Chem.*, *7* (1973) 374.
7 W. B. England, S. H. Liu and H. W. Myron, *J. Chem. Phys.*, *60* (1974) 3760.
8 J. Nakahara, H. Franzen and D. K. Misemer, *J. Chem. Phys.*, *76* (1982) 4080.
9 S. H. Liu, W. B. England and H. W. Myron, *Solid State Commun.*, *14* (1974) 1003.
10 W. B. Pearson, *A Handbook of Lattice Spacings and Structures of Metals and Alloys*, Pergamon Press, New York, 1958.
11 F. Grønvold, H. Haraldsen, B. Pedersen and T. Tufte, *Rev. Chim. Miner.*, *6* (1969) 215.
12 A detailed discussion of the crystal structures may be found in A. Kjekhus and W. B. Pearson, *Prog. Solid State Chem.*, *1* (1964) 83; F. Hulliger, *Struct. Bonding (Berlin)* *4* (1968) 83.

13 M. Lax, *Symmetry Principles in Solid State and Molecular Physics*, Wiley-Interscience, New York, 1974.

14 H. F. Franzen and G. A. Sawatzky, *J. Solid State Chem.*, *15* (1975) 229.

15 I. Tsubokawa, *J. Phys. Soc. Jpn.*, *14* (1959) 196. (See also ref. 11.)

16 See for example, T. Hughbanks and R. Hoffmann, *J. Am. Chem. Soc.*, *105* (1983) 3528; M. Kertesz and R. Hoffmann, *J. Am. Chem. Soc.*, *106* (1984) 3453.

17 N. W. Ashcroft and N. D. Mermin, *Solid State Physics*, Holt, Rinehart and Winston, New York, 1976.

18 W. A. Harrison, *Solid State Theory*, Dover, New York, 1980.

19 U. Öpik and M. H. L. Pryce, *Proc. R. Soc. London, Ser. A*, *238* (1957) 425.
    R. F. W. Bader, *Can. J. Chem.*, *40* (1962) 1164.

20 For a discussion of the experimental facts see: K. Selte and A. Kjekshus, *Acta Chem. Scand.*, *27* (1973) 3195.

21 R. E. Peierls, *Quantum Theory of Solids*, Oxford University Press, London, 1955.
    M.-H. Whangbo, *Acc. Chem. Res.*, *16* (1983) 95.

22 TiS: H. Hahn and B. Harder, *Z. Anorg. Allg. Chem.*, *288* (1956) 241.

23 CrS: T. Kamigaichi, K. Masumoto and T. Hihara, *J. Phys. Soc. Jpn.*, *15* (1960) 1355.

24 H. F. Franzen, D. H. Leebrick and F. Laabs, *J. Solid State Chem.*, *13* (1975) 307.

25 W. Tremel, R. Hoffmann and J. Silvestre, to be published.

Appendix A

The calculations were performed using the extended Hückel method within the tight-binding approximation [A1]. The density of states calculations were obtained with the use of 28 k points [A2] for the hexagonal phase and a 36 k point set for the orthorhombic geometry. The coordinates and other geometrical data were extracted from the literature and references given in the main body of the text.

TABLE A1

Extended Hückel parameters [A5, A6]

Orbital	H_{ii} (eV)	ζ [a]	ζ_2	C_1 [a]	C_2
V 3d	-8.67	4.75	1.70	0.4755	0.7052
V 4s	-7.95	1.25			
V 4p	-4.51	1.28			
S 3s	-20.0	1.82			
S 30	-13.3	1.82			

[a]Coefficients and exponents in double zeta expansion.

The diagonal elements H_{ii} are listed in Table A1 along with the orbital exponents and coefficients. For vanadium, a charge iteration procedure [A3] was used to generate the valence state ionization potentials. The H_{ij} values were computed with the weighted H_{ij} formula [A4].

References for Appendix A

A1 M.-H. Whangbo, R. Hoffmann and R. B. Woodward, *Proc. R. Soc. London, Ser. A*, *366* (1979) 23.

A2 J. D. Pack and J. J. Monkhorst, *Phys. Rev. B, 16* (1977) 1748.
A3 C. J. Ballhausen and H. B. Gray, *Molecular Orbital Theory*, W. A. Benjamin, New York, 1964.
A4 J. H. Ammeter, H.-B. Bürgi, J. C. Thibeault and R. Hoffmann, *J. Am. Chem. Soc., 100* (1978) 3686.
A5 J. W. Richardson, R. R. Powell and W. C. Nieuwport, *J. Chem. Phys., 38* (1963) 796.
A6 D. M. Hoffman and R. Hoffmann, *J. Am. Chem. Soc., 104* (1982) 3858.